Mechanism of vacuum breakdown in radio-frequency accelerating structures

S. A. Barengolts,[1,4,*] V. G. Mesyats,[1] V. I. Oreshkin,[2,3] E. V. Oreshkin,[4]
K. V. Khishchenko,[5] I. V. Uimanov,[6] and M. M. Tsventoukh[4]

[1]*Prokhorov General Physics Institute, RAS, 119991 Moscow, Russia*
[2]*Institute of High Current Electronics, Siberian Branch, RAS, 634055 Tomsk, Russia*
[3]*National Research Tomsk Polytechnic University, 634050 Tomsk, Russia*
[4]*Lebedev Physical Institute, RAS, 119991 Moscow, Russia*
[5]*Joint Institute for High Temperatures, RAS, 125412 Moscow, Russia*
[6]*Institute of Electrophysics, Ural Branch, RAS, 620016 Ekaterinburg, Russia*

(Received 12 September 2017; published 12 June 2018)

It has been investigated whether explosive electron emission may be the initiating mechanism of vacuum breakdown in the accelerating structures of TeV linear electron-positron colliders (Compact Linear Collider). The physical processes involved in a dc vacuum breakdown have been considered, and the relationship between the voltage applied to the diode and the time delay to breakdown has been found. Based on the results obtained, the development of a vacuum breakdown in an rf electric field has been analyzed and the main parameters responsible for the initiation of explosive electron emission have been estimated. The formation of craters on the cathode surface during explosive electron emission has been numerically simulated, and the simulation results are discussed.

DOI: 10.1103/PhysRevAccelBeams.21.061004

I. INTRODUCTION

At present, intense work is underway to develop a TeV electron-positron collider in the framework of international cooperation on the creation of the Compact Linear Collider (CLIC) [1]. The CLIC accelerating structure, made of copper, operates in the X band, namely at 11.994 GHz. In a system of this type, the particle-accelerating field strength is limited by vacuum breakdown, which may occur over the surface of the accelerating structure. The initiation of breakdown is accompanied by a sharp increase in the emission current from the structure surface, which may reach tens or even hundreds of amperes. As this takes place, a portion of the electromagnetic wave power is absorbed, resulting in a decrease in particle acceleration rate. In addition, the breakdown erodes the walls of the accelerating structure and, hence, impairs its long-term performance. The maximum accelerating field achieved by now is 100 MV/m, which gives rise to a macroscopic electric field over 200 MV/m at the surface of the accelerating structure [2].

The initiating mechanism of vacuum breakdown in rf accelerating structures is the subject of studies aimed at improving the stability of operation of the structures and at seeking ways for enhancing the accelerating electric field. These studies have been carried out since the development of the linear collider; however, the mechanism of vacuum breakdown in the CLIC accelerating structures still remains obscure [2–6].

Nevertheless, recently a number of important experimental results have been obtained which, in our opinion, make a significant contribution to the understanding of the physical processes underlying the rf conditioning of the surface of an accelerating structure [4–6]. In particular, two types of breakdown were observed [4–5]: "normal breakdown" (NL-BD), which occurred after operation over many pulses without breakdown, and "following-pulse breakdown" (FP-BD), which occurred at the first pulse following the breakdown pulse and was spatially linked with the latter, i.e., occurred at the same place. Analysis of the conditioning of several structures tested at KEK and CERN revealed clear evidence that the conditioning progressed with number of rf pulses and not with number of breakdowns [6]. Finally, a statistical examination of experimental results on rf and dc vacuum breakdowns [5] indicated a similar vacuum breakdown mechanism for these types of breakdown.

In this paper, the rf breakdown mechanism is analyzed based on the results of previous experimental studies of pulsed breakdown in vacuum [7,8]. In those experiments, rectangular pulses of high voltage (from tens to hundreds of

*sabarengolts@mail.ru

kilovolts) and duration from one nanosecond to several microseconds were used. The electrode gap spacing was varied from hundreds of micrometers to several centimeters. The vacuum breakdown characteristics were investigated for a variety of electrode materials (W, Cu, Al, Mo, Pb, several grades of graphite, etc.) and for different cathode geometries (planes, hemispheres, cones, etc.). The use of nanosecond voltage pulses made it possible to minimize the contribution of slow processes (adsorption, diffusion, migration, etc.) and secondary (anode) processes to the development of vacuum breakdown.

As shown experimentally, the failure of vacuum insulation under the action of nanosecond voltage pulses is due to the occurrence of cathode plasma microblobs (cathode flares). Expansion of the cathode flares into the electrode gap is accompanied by an increase in the current emitted from the cathode. This phenomenon is called explosive electron emission.

A detailed investigation of explosive electron emission has shown that the cathode material turns into plasma due to intense energy release in microscopic regions on the cathode surface. In the case of vacuum breakdown occurring at nanosecond voltage pulses, the energy is concentrated mainly due to the resistive heating of cathode microprotrusions by high-density field emission current. The plasma formed at the cathode as a result of explosions of the microprotrusions expands with high velocity ($\sim$10 km/s) into the electrode gap. The electron emission from the cathode compensates the runaway of electrons from the plasma boundary. The emission sites grow in number during the discharge due to the interaction of the high-density erosion plasma with the cathode surface. Eventually, cathode flares cover a larger and larger cathode region, giving rise to a sharp increase in emission current in the vacuum diode. The operation of cathode flares results in the formation of micrometer-sized craters on the cathode.

The study of explosive electron emission in a vacuum diode [8] has made it possible to clearly distinguish three stages in the development of a pulsed vacuum discharge. During the first stage (vacuum breakdown), energy is concentrated in microregions of the cathode surface, giving rise to plasma formation in these regions. The second (spark) stage is accompanied by an increase in the current passage area on the cathode, expansion of cathode flares into the electrode gap, and an increase in diode current. The third (arc) stage starts as soon as the electrode gap becomes filled up with plasma.

There are two main factors indicating that the physical processes involved in pulsed vacuum breakdowns and in breakdowns taking place in the CLIC accelerating structures are common in nature. These are the sharp current rise after breakdown initiation and the type of damage to the electrode surface (micrometer-sized craters) observed after the discharge operation [2]. Previously, the explosive electron emission initiated on the surface of the slow-wave structure of a microwave oscillator was pointed out as the cause for the limitation of the microwave pulse duration [9,10].

The paper is arranged as follows: The first part considers the physical processes that occur in a vacuum breakdown at a dc electric field, and the delay time to breakdown is shown to be related to the voltage applied to the diode. Next, based on the results of this consideration, the development of a vacuum breakdown in an rf electric field is analyzed and the main parameters responsible for the initiation of explosive electron emission are estimated. The concluding part presents the results of a numerical simulation of the crater formation on a cathode during explosive electron emission.

II. PARAMETERS OF A DC VACUUM BREAKDOWN

Before proceeding to an analysis of the physical processes involved in an rf breakdown, let us consider a pulsed dc breakdown in vacuum. In our opinion, these types of breakdown proceed by the same mechanism that relies on the buildup of thermal instability in the cathode microprotrusions due to the prevalence of Joule heating over emissive cooling and heat removal to the bulk cathode [7,8,11,12]. The important role of cathode microprotrusions and of the associated electric field enhancement in the development of rf vacuum breakdown is indicated in [3,13,14].

However, the interpretation of the contribution of cathode microprotrusions to vacuum breakdown may be different. In particular, Timko *et al.* [15] first simulated the development of a vacuum discharge from the initiation of field emission to the transition to a vacuum arc using modern computer simulation methods. The shapes and fall times of current and voltage curves obtained in the context of the proposed model provided a good interpretation of the dc spark experiments [2]. However, the breakdown time chosen for the simulation ($\sim$3 ns) was too short compared with the typical breakdown times (tens of nanoseconds) measured in the experiments [2]. A cathode microprotrusion was modeled by a site of area 10^4 nm^2 on a plane cathode. To calculate the emission current density, the field enhancement factor $\beta = 35$ was assigned to this site. Together with the emission current, a neutral atom flux was specified which was rigidly bound, without any physical substantiation, with the current. Obviously, this flux should significantly reduce β and, eventually, be responsible for complete vaporization of an actual microprotrusion only due to electron emission. Besides, the calculations used an obviously overestimated coefficient of sputtering of the cathode surface, suggesting its bombardment with keV energy ions. However, the ion energies in the cathode spot zone of a vacuum discharge are lower by almost 2 orders of magnitude [7,16].

The distinctive feature of the explosive emission approach that we use in the present work is the assumption

that a cathode microprotrusion disintegrates as a result of intense heating by emission current. The heating of cathode microprotrusions receives mention in [15], but it, quite reasonably, could not be considered for the protrusion geometry at hand. Nevertheless, the existence of a critical electric field at which a microprotrusion is heated in an avalanche-like manner is discussed in another paper [17] co-authored by some of the authors of the study [15].

As mentioned above, the approach that we propose here relies on the results of pulsed vacuum breakdown studies [7]. To investigate the vacuum breakdown characteristics under controlled conditions, a series of experiments was performed with classical needle field emitters. The needles were prepared from electrochemically etched metal wires of diameter 0.1–0.8 mm. This technique provided needle tip radii of 100–500 nm. The copper needles were additionally electropolished. For each emitter, a dc Fowler–Nordheim characteristic was obtained. The voltage pulse duration was varied from 0.7 ns to 4 μs. The shorter was the pulse, the higher the voltage required to initiate breakdown. The breakdown delay time was recorded as soon as the emission current started sharply rising.

Experimental investigations of the vacuum breakdown mechanism for needle cathodes have revealed a relationship between the delay time to breakdown initiation t_d and the current density at the cathode j, which can be described as [7]

$$j^2 t_d = \text{const}. \tag{1}$$

The same relation was obtained for plane cathodes for breakdown delay times ranging from several nanoseconds to tens of nanoseconds [7].

The solution of the nonstationary problem of the heating of a needle cathode by thermal field emission current has shown that the resistive heating of the cathode is the main mechanism by which heat is released within a few to tens of nanoseconds [18]. The Nottingham effect is appreciable but not dominant in the heating dynamics. The numerical simulation has yielded the following form of relation (1):

$$j^2 t_d = f \frac{\rho c_p}{\kappa_0} \tag{2}$$

where ρ is the density of the cathode material, c_p is the specific heat, and κ_0 is the temperature coefficient of resistivity defined by $\kappa = \kappa_0 T$. For a cone-shaped microprotrusion with small cone angle, the factor f slightly depends on geometry (cone angle and tip radius) and is determined mainly by the temperature at which breakdown is initiated. For this temperature, the melting temperature, boiling temperature, or critical temperature was taken [7,8,11,12,18].

To derive a criterion for breakdown initiation, we use the analogy between the explosion of cathode microprotrusions and the electrical explosion of wires [7,8]. The use of this analogy is validated by that in both cases, the main mechanism of heat release in a microprotrusion (thin wire) is its resistive heating by high-density current, resulting in an explosive metal-to-plasma transition. An important characteristic of a wire explosion is the integral of specific current action [19] defined by

$$\bar{h} = \int_0^{t_d} j^2 dt. \tag{3}$$

The quantity $\bar{h}$, which characterizes the energy stored in the wire prior to its explosion, slightly depends on current density in the range around 10^8 A/cm^2. In view of this, relation (1) can be rewritten as

$$j^2 t_d \approx \bar{h}. \tag{4}$$

For copper, $\bar{h} = 4.1 \times 10^9$ A^2 s/cm^4 was measured [8]. This value will be used for estimates in the subsequent discussion.

The pulsed vacuum breakdown investigations performed with plane cathodes have revealed that at high electric fields at the cathode surface [7], the delay time to breakdown depends on the field not exponentially but as a power function, $t_d \propto (E_{\text{av}})^p$, with $p \cong -3$, where E_{av} is the macroscopic field at the cathode. For plane-parallel electrodes, we have $E_{\text{av}} = U/d$, where U is the voltage across the diode and d is the electrode gap spacing. The power-law dependence of the breakdown delay time on electric field is due to the effect of the space charge of emitted electrons [20]. This effect is responsible for the fact that the prebreakdown current density obeys the three-halves power law:

$$j_{3/2} = \frac{1}{9\pi} \left(\frac{2e}{m_e} \right)^{1/2} \frac{U^{3/2}}{d_{\text{eff}}^2}, \tag{5}$$

where e and m_e are the electron charge and mass, respectively, and d_{eff} is the effective gap spacing defined as $d_{\text{eff}} = U/(\beta \cdot E_{\text{av}})$, where β is the factor of field enhancement at the cathode surface microprotrusions.

To estimate the electric field at the microprotrusion tips, E_0, in view of the space charge of emitted electrons, we use a one-dimensional approximation (the range of its applicability is discussed below). The equation for finding the electric field at the tip of a cathode microprotrusion under the conditions of field emission reads as [20]

$$\begin{aligned} &4kAU^{3/2} \exp(-B/E_0) - 3U \\ &\quad = 9k^2 A^2 E_0^2 d_{\text{eff}}^2 \exp(-2B/E_0) - 3E_0 d_{\text{eff}}, \end{aligned} \tag{6}$$

where A and B are the coefficients in the Fowler–Nordheim equation $j_{\text{FN}} = AE_0^2 \exp(-BE_0)$, and $k = 2\pi(2m_e/e)^{1/2}$.

Next we discuss the results of a dc vacuum breakdown experiment [21] invoking the above results of pulsed vacuum breakdown studies. In the experiment [21], the cathode material and treatments were the same as in the rf breakdown experiment [2]. Both electrodes were made of pure copper (Cu OFE, UNS C10100). The anode was a hemispherical rounded tip, 2.3 mm in diameter, and the

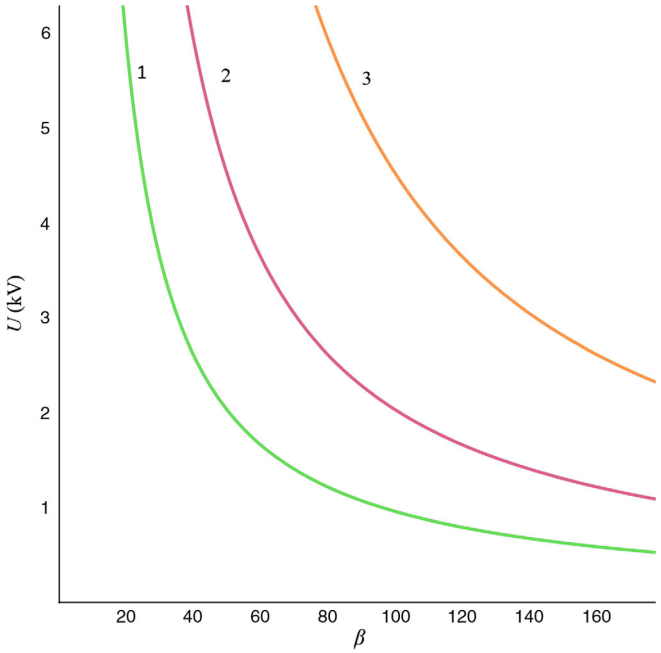

FIG. 1. Breakdown voltage U versus field enhancement factor β for a 50-ns delay time and a varied electrode gap spacing: $d = 10$ (curve 1), 20 (curve 2), and 40 μm (3).

cathode was a grounded 10×50 mm rectangular plane surface. The electrode gap spacing d was varied from 10 to 50 μm; most of the shots were performed with $d = 20$ μm. The dc breakdown field was measured, and the field enhancement factor β was estimated using Fowler–Nordheim characteristics. The measurements were performed not only in a "conditioning mode" where the field was increased until breakdown occurred, but also in a "breakdown rate mode" where the working field was kept constant. Besides these basic experiments, additional information about the breakdown mechanism was obtained by measuring the breakdown delay time. The voltage pulse duration was 1–2 s and the voltage rise time was about 100 ns.

The average vacuum breakdown characteristics obtained in the experiment [21] that will be used in the subsequent discussion are the following: average field enhancement factor $\beta = 77$, average breakdown field $\beta E_{\mathrm{av}} = 10.8$ GV/m, and breakdown delay time (minus diode voltage rise time) $t_d \approx 50$ ns.

Figure 1 presents the breakdown voltage across the diode as a function of electric field enhancement factor β for different values of the electrode gap spacing. The curves were obtained using relation (4) for $t_d = 50$ ns. The electric field entering into the Fowler–Nordheim equation was calculated using relation (6). As can be seen from the plots, for the typical experimental conditions [21], the quantity βE_{av} ranges from 11.2 GV/m (at $U = 6$ kV) to 10 GV/m (at $U = 2$ kV) irrespective of the gap spacing; that is, it is in rather good agreement with experimental data (in the experiment [21], the standard deviation of the breakdown field βE_{av} from the average value $\beta E_{\mathrm{av}} = 10.8$ GV/m was 16%). The slight increase in βE_{av} with decreasing β is due to the increasing effect of the space charge of emitted electrons. The obtained threshold value of β, such that at its higher values breakdown is initiated, is almost equal to 48, the threshold value determined experimentally for $E_{\mathrm{av}} = 225$ MV/m [21] (see Fig. 1, the data for $d = 20$ μm and $U = 4.5$ kV).

Thus, the estimates obtained merely from experimental data on pulsed vacuum breakdown describe rather well the experimental data on the dc breakdown for the materials used in the CLIC accelerating structures. Next, using the results obtained here, we estimate the characteristics of the vacuum breakdown in rf electric fields.

III. VACUUM BREAKDOWN INITIATION IN RF ACCELERATING STRUCTURES

The mechanism of vacuum breakdown in rf electromagnetic fields has not yet been adequately investigated theoretically. Mesyats [9] proposed an explosive emission mechanism of vacuum breakdown between electrodes subject to the action of microwave fields. According to this mechanism, breakdown occurs due to the heating of microprotrusions by the emission current during the negative half-wave of the cathode voltage. For a cylindrical protrusion with a small radius-to-height ratio, not taking into account the thermal conductivity of the metal and the temperature dependence of its resistivity, a simple formula has been derived for the time it takes for the protrusion to be heated to the triple point temperature:

$$t = \frac{(T - T_0)\rho c_p}{\nu j^2 \kappa t_j} \tag{7}$$

where ν is the microwave frequency and t_j is the duration of the emission current in the oscillation half-period. For $j = 10^9$ A/cm^2 and the microwave frequency equal to 10 GHz ($t_j \approx 2 \times 10^{-11}$), the time in which the protrusion will be heated to the melting temperature is estimated to be of the order of 10^{-8} s. The governing part of field emission processes in the development of a vacuum breakdown in an rf accelerating structure was demonstrated by Wang and Loew [13].

The heating of a single emitter by the field emission current is given in [9]. The existence of individual emission centers on the surface of accelerating structures of varied geometry with varied field enhancement factors shows up, in particular, in the occurrence of dark current [2]. According to the estimating formulas (7), current density is a key parameter which determines the development of vacuum breakdown. Therefore, it is reasonable to suppose that, in view of the exponential behavior of field emission current density, a considerable contribution to the initiation of breakdown is made by cathode microprotrusions having

the highest field enhancement factor. The time dependence of field emission current density is somewhat weaker than the exponential for high current densities at which the space charge of emitted electrons affects the emission process. However, in this case, with Joule heating as the dominant heating mechanism, we have a strong dependence of the heating time on β: $t \sim \beta^{-4}$. Therefore, breakdown is initiated at certain sites rather than at all emission centers simultaneously.

A numerical simulation of the heating of a conical microprotrusion by emission current, performed in a two-temperature (electrons and phonons) statement taking into account the Nottingham effect, has shown that the microprotrusion can be heated to the melting temperature within tens of nanoseconds if the amplitude of the electric field at the microprotrusion is ~10 GV/m [22]. In this case, the time of heating to the melting temperature t_m is related to the current density, like in the case of pulsed breakdown, as

$$j_{\mathrm{av}}^2 \cdot t_m = \mathrm{const}, \tag{8}$$

where j_{av} is the current density averaged over the rf field oscillation period. Relation (8) holds throughout the gigahertz range of frequencies except the cases when breakdown occurs within the first few oscillation periods of the electric field. Relation (8) depicts the fact that the main mechanism of heat release in the microprotrusion is the resistive heating by emission current.

Keser *et al.* [14], having analyzed the mechanism of heating of a microprotrusion in an rf electric field, arrived at a different conclusion. According to their estimates, the Nottingham effect makes a major contribution to the heating of a microprotrusion, whereas Joule heating contributes only a few percent. The difference in the results of the studies [14,22] is due to different microprotrusion geometries. The authors of [14] analyzed a cone microprotrusion with a small emission area and a large cone angle. This type of protrusion is heated insignificantly, even though the current density can be as high as above 10^9 A/cm^2, as demonstrated in the experiment [23].

Before analyzing experimental data on the vacuum breakdown in rf accelerating structures, we should note the following: An essential feature required of a CLIC accelerating structure is that at an accelerating field of 100 MV/cm and a nominal pulse duration, the breakdown rate must be lower than 3×10^{-7} per pulse per meter of structure [24]. Breakdown rate (BDR) is the probability that breakdown will occur during any given pulse. It is determined experimentally by divining the number of breakdowns by the total number of rf pulses during an operation period. In this connection, significant efforts were made to investigate the dependence of BDR on an accelerating field and on rf pulse duration. In these investigations, unlike in pulsed vacuum breakdown experiments [7], the surface microprotrusions responsible for rf breakdown initiation could be formed during rf pulses which did not cause breakdown. This is obviously related to the rf magnetic field that heats the structure surface. The heating can induce the formation of surface microcracks and microprotrusions [25], which are potential emission centers with high field enhancement factors β, promoting breakdown initiation. As a consequence, BDR increases as the structure surface is more and more heated [26,27]. We do not consider these processes because the focus of our study is on the rf breakdown per se.

By now two criteria for the initiation of vacuum breakdown in rf fields have been found experimentally [2,3]. The first criterion relates BDR with electric field amplitude E_A:

$$E_A^{30}/\mathrm{BDR} = \mathrm{const}. \tag{9}$$

The second criterion relates E_A and t_p for a constant BDR:

$$E_A \cdot t_p^{1/6} = \mathrm{const}. \tag{10}$$

Let us briefly analyze the empirical relations (9) and (10). Obviously, if relation (9) describes a (sharp) increase in the probability of breakdown with electric field amplitude, relation (10) should describe the dependence of E_A on the delay time to breakdown. Relation (10) implies a probability of breakdown during an rf pulse if the breakdown delay time ("breakdown timing," in the terminology of [4]) is not greater than the pulse duration. For a rather large number of "normal breakdowns" (NL-BD), these times are uniformly distributed over the rf pulse. Hence, for a breakdown to occur during an rf pulse, the condition $t_d \le t_p$ must be fulfilled. As the delay time is related to the field enhancement at the surface of an accelerating structure, to its maximum value, $t_d \approx t_p$, there should correspond a minimum value of the field enhancement factor, $\beta_{\mathrm{threshold}}$, at which breakdown is possible. The empirical relation (10) reflects the fact that $\beta_{\mathrm{threshold}}$ is invariable for this relation between electric field and pulse duration. Hence, in this case, the conditions for a breakdown to occur remain unchanged, and the probability of breakdown is 100% if $\beta \ge \beta_{\mathrm{threshold}}$. Violation of this relation would lead to a change in $\beta_{\mathrm{threshold}}$ and, as a consequence, in BDR, in view of its strong field dependence [see relation (9)].

Next, we used the results of the study [22] to estimate the relationship between the breakdown delay time and the macroscopic field at the surface of an accelerating structure for oscillation frequencies ranging up to 10 GHz. We considered a diode with plane-parallel electrodes whose parameters were taken the same as in [21]. The amplitude of the voltage $U = U_A \sin(\omega t)$ applied to the diode was chosen so that the maximum macroscopic field at the cathode, $E_A = U_A/d$, be some hundreds of volts per meter. The breakdown delay time was calculated using relation (4) with the current density averaged over the rf field oscillation period, j_{av}.

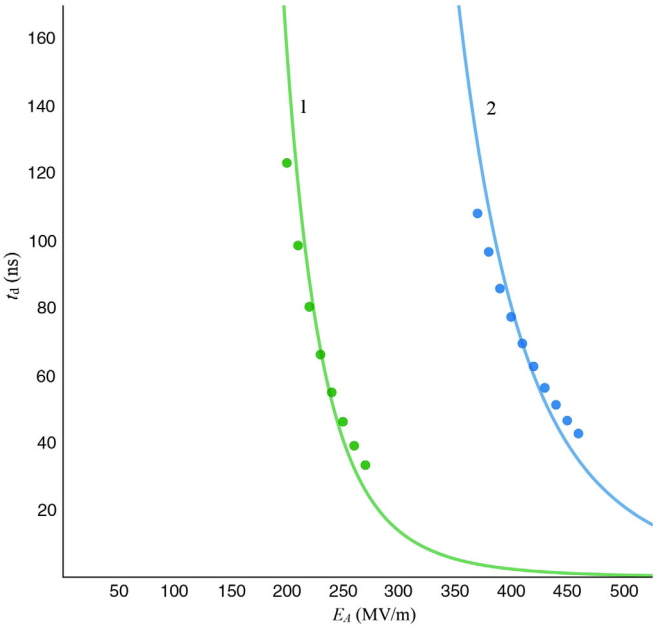

FIG. 2. Delay time t_d as a function of the electric field amplitude E_A, at the surface of an rf accelerating structure for different values of the field enhancement factor: $\beta = 77$ (1) and 50 (2); curves represent the relation $t_d(\beta_{\text{threshold}}) \propto E_A^{-6}$ and the electric field oscillation frequency $\nu = 10$ GHz.

It should be noted that the numerical simulation [22] did not consider the effect of the space charge of emitted electrons on the electric field at the microprotrusion tip. Therefore, according to the calculations, the heating time t_m decreased exponentially with rf electric field amplitude. In the present study, the effect of the space charge of emitted electrons was taken into account according to the above procedure used for a dc breakdown. The approach used to study the electron emission in dc fields is quite applicable to the case of rf fields, as the electron tunneling time in field emission is 10^{-15} s [28], which is 2 orders of magnitude shorter than the oscillation period of the electric field. An experimental studies of field emission in rf fields has demonstrated that this phenomenon can be adequately described using the Fowler–Nordheim theory [29].

The calculation results are presented in Fig. 2. The calculations were performed for two values of the field enhancement factor: $\beta_{\text{threshold}} = 77$, equal to the average value obtained in the study [21], and, for comparison, $\beta_{\text{threshold}} = 50$.

For the proposed CLIC parameters described in [24], it is expected that at an accelerating electric field amplitude of 100 MV/m, the rf pulse duration will be 156 ns and the electric field at the surface will be lower than 260 MV/m. According to the plots given in Fig. 2, for the field at the cathode equal to 250 MV/m and the rf pulse duration $t_p = 150$ ns, breakdown may occur at $\beta > \beta_{\text{threshold}} \approx 70$. The values of β typical of rf structures are in the range 30–60 [2,30]. These values were obtained using the Fowler–Nordheim characteristics for dc modes with low emission currents. We, however, are interested in the values of β that occur immediately before a breakdown-initiating pulse. It is reasonable to suppose that for breakdown to be initiated, microirregularities must be present on the surface whose field enhancement factors would be greater than β typical of no-breakdown cases, and this is consistent with our estimates. It is possible that microirregularities with anomalously high field enhancement factors are responsible for the vacuum breakdowns in the CLIC accelerating structures. It must be emphasized that these are the least field enhancement factors at which $t_d \approx t_p$; that is, a significant proportion of breakdowns detected in experiments are initiated at microirregularities with much greater β. This is especially the case with FP-BD breakdowns [4], which occur, for the most part, early in an rf pulse. The origin of microirregularities of this type still remains obscure, as microprotrusions with such a small tip-radius-to-height ratio can hardly be imagined. Anyhow, high-resolution imaging of accelerating structures failed to detect such microprotrusions on their surfaces (see, e.g., [2]).

It is also conceivable that in the case under consideration, two factors are effective: the presence of microprotrusions that provide intense field enhancement and a local decrease in work function the reason of which is not yet clear. Nevertheless, the above analysis did not take into account the geometric factor; however, at local fields βE_A of the order of 15 GV/m, microprotrusions showing high emissivity will inevitably be heated to high temperatures by field emission current.

The calculation results presented in Fig. 2 also match rather well the empirical relation (10): $t_d(\beta_{\text{threshold}}) \approx t_p \propto E_A^{-6}$. At the same time, the simple model under consideration, though providing some agreement with experimental data, fails to characterize quantitatively an rf vacuum breakdown. In particular, according to estimates, the space charge of emitted electrons is localized within $\sim 2 \times 10^{-6}$ cm from the cathode [20]. For microprotrusions of tip radius $<10^{-5}$ cm (such as those present on the walls of the accelerating structures [2]), the one-dimensional approximation, disregarding dimensional effects, yields an underestimated value of the electric field. Thus, according to the electric field estimates obtained using a two-dimensional model for microprotrusions of tip radius 10 nm, the effect of the space charge of emitted electrons becomes meaningful at $\beta E_{\text{av}} > 9$ GV/m [26]. When calculating the emission current, one must also consider the increase in effective emission area with electric field and temperature [31,32].

A more rigorous analysis of the initiation of rf vacuum breakdown is needed to perform a self-consistent solution of the two-dimensional problem of the heating of a microprotrusion by the electrons emitted from its surface [33]. Nevertheless, we believe that the above estimates demonstrate the probability that a vacuum breakdown in an rf electric field may be initiated due to the heating of microprotrusions by electron emission current.

IV. FORMATION OF A CRATER ON THE CATHODE SURFACE DUE TO THE EXPLOSION OF A MICROPROTRUSION

As mentioned above, the proposed breakdown mechanism is also supported by the experimental examinations of the electrode surfaces after rf and dc breakdowns. According to these examinations, the craters formed on the surfaces are identical for both types of breakdown [2].

Let us illustrate the crater formation due to the explosion of a cathode microprotrusion by results of numerical simulations. As mentioned above, owing to the high emission current density, the explosion of a microprotrusion is similar to the explosion of a thin wire. Based on this similarity, models of explosive emission processes have been constructed that not only explained the mechanism of vacuum breakdown initiation but also revealed the main characteristics of the near-cathode and plasma processes that occur during the spark stage of a vacuum discharge [34–37]. In the most rigorous statement assuming a continuous metal-to-plasma transition, the problem of the explosive destruction of a microprotrusion on a copper cathode was solved by Shmelev and Litvinov [36,37]. The calculations were performed for the current range 3–7 A. In a general outline, the predicted scenario of the electrical explosion of a microprotrusion on a cathode is the following: Owing to the high current density, intense Joule heat release in the microprotrusion results in fast heating of its tip and in a sharp rise of the pressure that reaches several hundreds of kilobars within a short time. This pressure gives rise to a destruction wave propagating toward the microprotrusion base. At the same time, a completely ionized plasma (plasma flare), whose initial electron temperature reaches 10 eV, expands in the opposite direction with a velocity higher than 10^6 cm/s. As this takes place, a continuous metal-to-plasma phase transition occurs in a layer of most intense heat release. In the study [36,37], the initial stage of the explosive destruction of a microprotrusion on a cathode was numerically simulated. The computations were carried out up to a time of the order of 1 ns. The results obtained were used subsequently to simulate the processes occurring in a plasma jet [38].

In the study presented here, the julia magnetohydrodynamic (MHD) code [39] was used. With this code, based on the particle-in-cell technique, the explosion of wires was previously simulated in a two-dimensional approximation (see, e.g., [40]). The system of MHD equations to be solved with the code consists of the hydrodynamics equations that describe the laws of conservation of mass, momentum, and energy

$$\frac{\partial \rho}{\partial t} + \nabla(\rho \mathbf{v}) = 0, \tag{11}$$

$$\rho \frac{\partial \mathbf{v}}{\partial t} + \rho \mathbf{v} \nabla \mathbf{v} = -\nabla p + \frac{1}{c} \mathbf{j} \times \mathbf{H}, \tag{12}$$

$$\frac{\partial \rho \varepsilon}{\partial t} + \nabla(\rho \varepsilon \mathbf{v}) = -p \nabla \mathbf{v} + \frac{\mathbf{j}^2}{\sigma} + \nabla(\lambda \nabla T). \tag{13}$$

Maxwell's equations are written in a quasistationary approximation (with no account of displacement currents)

$$\frac{1}{c} \frac{\partial \mathbf{H}}{\partial t} = -\nabla \times \mathbf{E}, \qquad \nabla \times \mathbf{H} = \frac{4\pi}{c} \mathbf{j}, \tag{14}$$

and Ohm's law

$$\mathbf{j} = \sigma \left(\mathbf{E} - \frac{1}{c} \mathbf{v} \times \mathbf{H} \right), \tag{15}$$

where ρ is the density of the material and $\mathbf{v}$ is its velocity; p, ε, and T are the material pressure, internal energy, and temperature; $\mathbf{H}$ is the magnetic field strength; $\mathbf{E}$ is the electric field strength in a fixed coordinate system; $\mathbf{j}$ is the current density; λ is the thermal conductivity, and σ is the electrical conductivity.

Equations (11)–(15) were solved in cylindrical coordinates (r, z) using the following algorithm: The equation of motion (12) was solved for each particle and then the average mass velocity and the material density were found by summation over all the particles. In this method, the continuity equation (11) holds true by itself due to the Lagrangian nature of the particles. The energy equations (13) and Maxwell's equations (14) were solved on a fixed Eulerian network, which was constructed at the start of computations and remained unchanged throughout the running time of the code.

Boundary conditions for the equations of motion (12) can be specified in terms of material velocity or pressure. When integrating Eqs. (12), the boundary condition at the material-vacuum interface was specified as $p = 0$, whereas the boundary condition at the center ($r = 0$) corresponded to the condition of axial symmetry, that is to zero radial velocity: $v_r = 0$. For the energy balance equation (13), the heat flux at the boundaries was set equal to zero, which corresponded to the absence of external heat sources and sinks. The boundary conditions for Maxwell's equations (14) were specified as the radial component of the electric field vector $E_r = 0$ at $r = 0$, $z = 0$, and $z = Z_{\max}$ and the azimuthal component of the magnetic field vector $B_\varphi = 0$ at $r = 0$ and $B_\varphi = 2I(t)/(cR_{\max})$ at $r = R_{\max}$, where $Z_{\max}$ and $R_{\max}$ are the maximum values of coordinate z and Eulerian network radius, respectively [the current carried by the microprotrusion, $I(t)$, was calculated by integrating network equations].

The semiempirical wide-range equations of state [41] used in the simulation took into account high-temperature melting and evaporation. The electrical characteristics and thermal conductivity of the metal were calculated using tabulated data on the conductivity of copper [42].

The problem was solved in the following statement: It was assumed that explosive electron emission had already been initiated, and, therefore, the current was determined

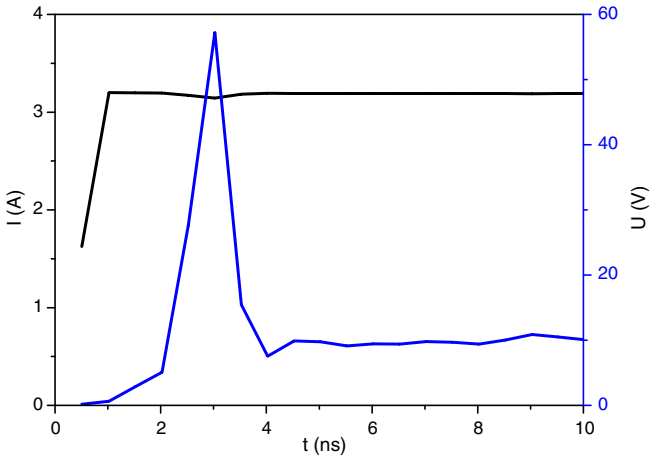

FIG. 3. Current and voltage waveforms.

by the parameters of the external circuit. The cathode-microprotrusion system was included in the electrical circuit, which was described by the equation

$$U_{\text{out}}(t) = I(t)R_{\text{out}} + U_{\text{load}}(t), \tag{16}$$

where $U_{\text{out}}(t)$ is the external source voltage, which increased to $U_0 = 3200$ V within 0.1 ns and then remained constant; $R_{\text{out}} = 1000\ \Omega$ is the external resistance, which was chosen so that the short-circuit current in the circuit was equal to 3.2 A, and $U_{\text{load}}(t)$ is the voltage across the load (cathode-microprotrusion system). The value of the current $I(t)$ was used for the boundary condition in solving Maxwell's equations (4). It was assumed that a microprotrusion shaped as a cylinder of radius 0.3 μm and length 1.5 μm was located on the surface of a plane copper cathode. The chosen current value 3.2 A corresponds to the current carried by an individual cell (ecton) of the cathode spot of a copper cathode vacuum arc [8].

Figure 3 shows the current and voltage waveforms obtained by solving numerically Eqs. (11)–(16). The voltage peak occurring within a few nanoseconds after the discharge initiation is due to the electrical explosion of the microprotrusion as a whole. A feature of the explosion is that the metal loses conductivity in the course of heating, as it changes from a solid to a plasma state. Subsequently, the voltage is stabilized at a level $U_{\text{load}} \approx 10$ V, which is the resistive drop caused by the current passing through the metal-plasma interface and through the computational domain of the cathode plasma. Accordingly, the power density "absorbed" by the material during the explosion, $j U_{\text{load}}$, reaches tens of W/μm^2.

The explosion of the microprotrusion under the action of an electric current [Fig. 4(a)] results in the production of a well-conducting, high-density cathode plasma, whose temperature reaches ~10 eV [see Fig. 4(b)]. As this takes place, a region of elevated pressure, which can reach several hundreds of kilobars, is formed near the cathode

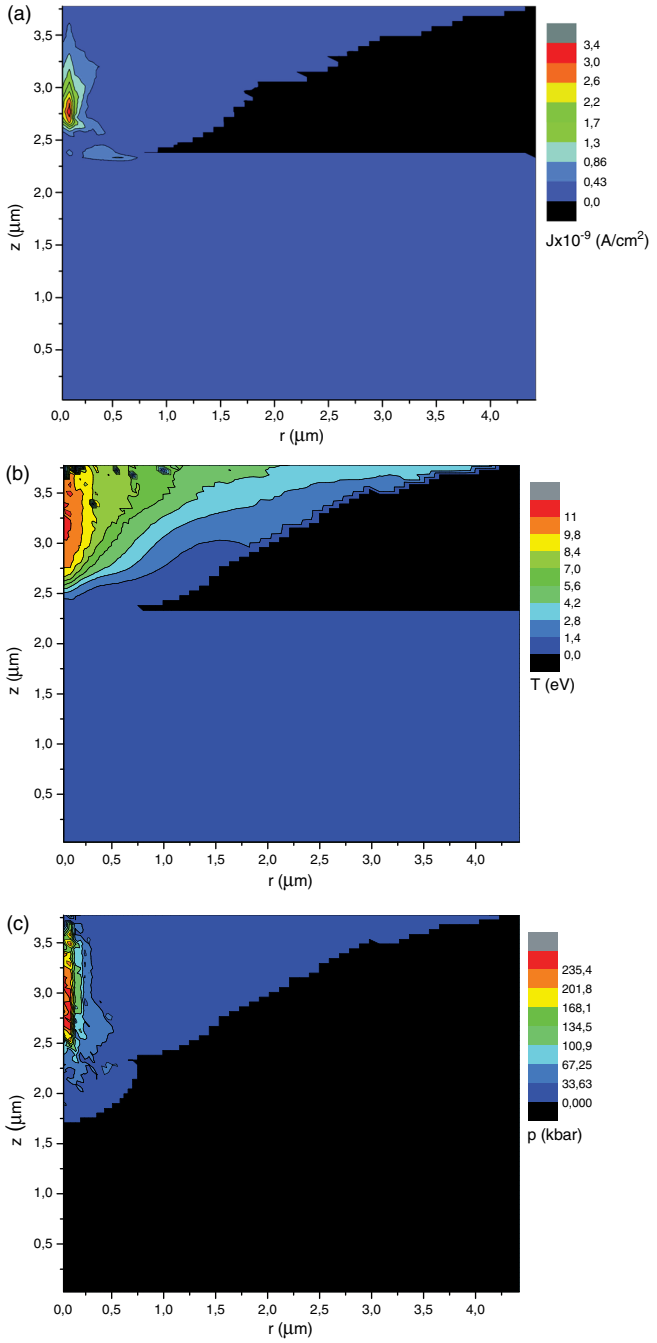

FIG. 4. Current density (a), temperature (b), and pressure distributions (c) at $t = 3$ ns.

surface [see Fig. 4(c)]. Under the action of this pressure, the molten metal is expelled from the pool formed as a result of the heating of the cathode surface region beneath the exploded microprotrusion [Fig. 5(a)]. The results obtained for the initial stage of the microprotrusion explosion agree with the results of the calculations [36,37].

The melt area increases with time due to the heating of the surface by the plasma produced as a result of the microprotrusion explosion. Eventually, a crater, several micrometers in radius, is formed on the cathode surface

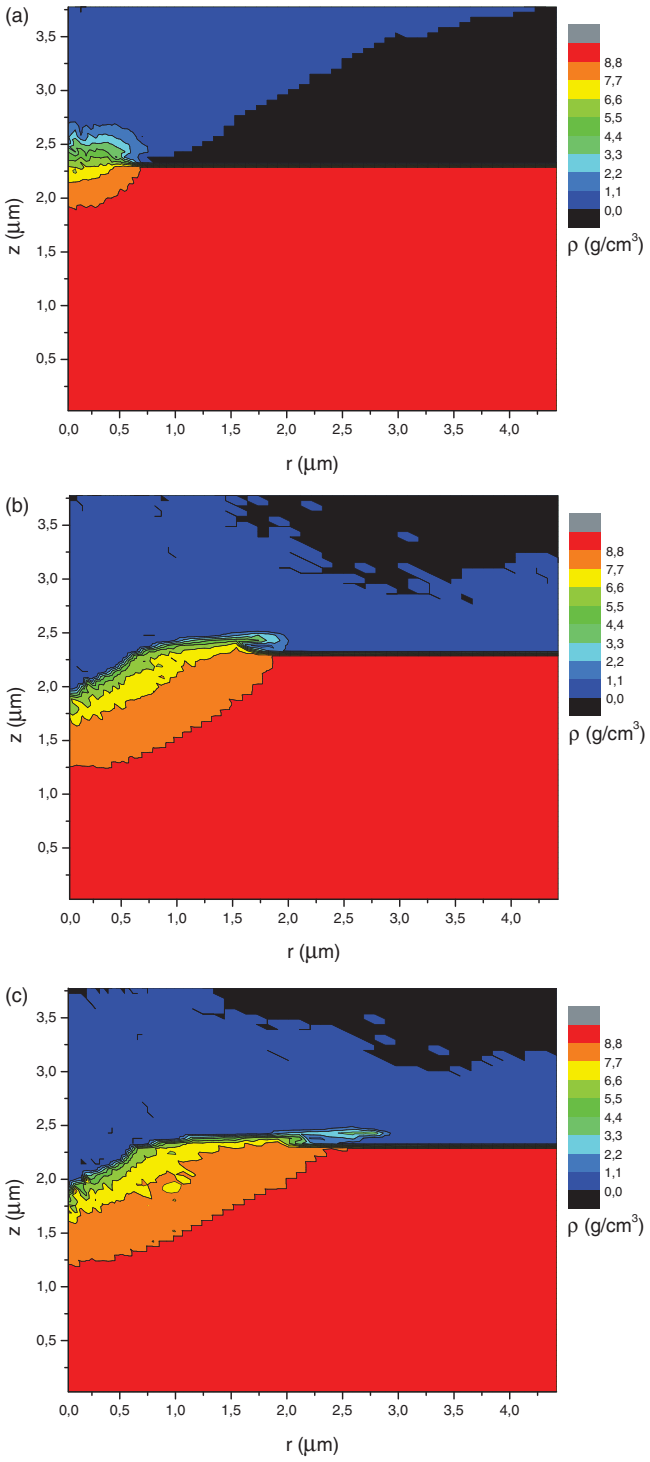

FIG. 5. Material density distribution at $t = 3$ (a), 5 (b), and 10 ns (c).

[see Figs. 5(b) and 5(c)]. The crater formation process is most intense during the first few nanoseconds after the discharge initiation. It should be noted that the above statement of the problem seems to be invalid for times over 5 ns, as it does not take account of the emissive processes at the metal-plasma interface. Therefore, Fig. 5(c) represents some illustrative hypothesis. Nevertheless, the calculations allow the conclusion that the estimated crater formation times and crater dimensions are consistent with the simulations of the process of crater formation in vacuum arcs [43–45]. This is not surprising if one takes into account the common mechanism of crater formation that involves high pressure and the existence of a dense plasma having a temperature of several electron volts at the metal-plasma interface.

Thus, the MHD calculations have shown that the electrical explosion of a microprotrusion having parameters typical of a single emission center (ecton) may result in the formation of a crater, several micrometers in radius, on the cathode surface.

A different crater formation mechanism in the arc and spark stages of a vacuum discharge is proposed in [46,47]. This mechanism implies, as that proposed in [15], the existence of a flow of ions or ion clusters, accelerated to keV energies at the metal-plasma interface, incident on the cathode. An energetic ion flow incident on the cathode can arise in the spark stage of a discharge only if the discharge becomes unstable, and the formation of this flow is due to the processes at the boundary of the expanding cathode plasma [8,48–50]. However, ions with these energies cannot arise in a vacuum arc, as the operating voltage of a vacuum arc is as low as tens of volts [8,16]. The most likely kinetic energy of vacuum arc ions measured for a copper cathode is 57.4 eV [16].

The cathode surface morphology is substantially affected by the liquid metal formed in the vacuum arc cathode spot and extruded from the spot operation zone. This makes the direct conditioning of electrodes by breakdowns inefficient if the applied voltage pulse duration is greater than the time to the formation of a liquid-metal pool and the time to the onset of the pool motion. The experiments [51,52] showed that the factor β can be substantially reduced only for breakdowns of duration <5 ns, which agrees with our calculations. This accounts for the results of the experiments [4,6] that have led to the conclusion that direct conditioning of an accelerating structure with rf breakdowns does not improve the conditioning state.

V. CONCLUSION

The estimates and numerical simulation results obtained in this study indicate, in our opinion, that explosive emission processes play a decisive part in an rf breakdown. This finding provides a rather clear scenario of the rf breakdowns developing in the CLIC accelerating structures.

The high emission current density resulting from the local electric field enhancement at cathode microprotrusions and, perhaps, from a decrease in work function is responsible for the heating of the microprotrusions followed by their electrical explosion. According to the results of our

numerical simulation of the explosion of a cathode microprotrusion, the absorbed power density in this process can be as high as tens of $W/\mu m^2$. Obviously, the only power source that can be responsible for the high power absorbed during a vacuum breakdown in a CLIC accelerating structure is rf electromagnetic field power. The power absorption rate increases sharply with the number of emission centers simultaneously operating on the cathode. It is highly plausible that this is the cause of the "missing power" or "missing energy" effect [2]. As this takes place, the incident rf electromagnetic wave starts reflecting from the expanding high-density plasma. The portion of reflected radiation increases with time while the plasma is filling the space between the electrodes.

To study the physical processes involved in an rf breakdown in more detail, it is necessary to solve a self-consistent problem that describes the heating of a cathode microprotrusion and the electron emission from the protrusion and to simulate the absorption and reflection of an rf electromagnetic wave in the CLIC accelerating structures in view of the initiation of explosive electron emission on their walls.

ACKNOWLEDGMENTS

This work was supported in part by the Russian Foundation for Basic Research (Grants No. 16-08-00604, No. 17-08-01282, and No. 16-08-00969) and by Russian Academy of Sciences under the Basic Research Program I.11P.

[1] *A 3 TeV e^+e^- Linear Collider Based on CLIC Technology*, edited by G. Guignard (CERN Report No. CERN 2000-008, 2000).

[2] W. Wuensch, CERN-OPEN-2014-028. CLIC-Note-1025, CERN, Geneva, 2013.

[3] A. Grudiev, S. Calatroni, and W. Wuensch, New local field quantity describing the high gradient limit of accelerating structures, Phys. Rev. ST Accel. Beams **12**, 102001 (2009).

[4] X. Wu, J. Shi, H. Chen, J. Shao, T. Abe, T. Higo, S. Matsumoto, and W. Wuensch, High-gradient breakdown studies of an X-band Compact Linear Collider prototype structure, Phys. Rev. Accel. Beams **20**, 052001 (2017).

[5] W. Wuensch, A. Degiovanni, S. Calatroni, A. Korsbäck, F. Djurabekova, R. Rajamäki, and J. Giner-Navarro, Statistics of vacuum breakdown in the high-gradient and low-rate regime, Phys. Rev. Accel. Beams **20**, 011007 (2017).

[6] A. Degiovanni, W. Wuensch, and J. Giner Navarro, Comparison of the conditioning of high gradient accelerating structures, Phys. Rev. Accel. Beams **19**, 032001 (2016).

[7] G. A. Mesyats and D. I. Proskurovsky, *Pulsed Electrical Discharge in Vacuum* (Springer, Berlin, 1989).

[8] G. A. Mesyats, *Cathode Phenomena in a Vacuum Discharge: The Breakdown, the Spark, and the Arc* (Nauka, Moscow, 2000).

[9] G. A. Mesyats, in *High Power Microwave Generation and Applications* (SIF, Bologna, Italy, 1992), p. 345.

[10] S. D. Korovin, G. A. Mesyats, I. V. Pegel', S. D. Polevin, and V. P. Tarakanov, Mechanism for microwave pulse shortening in a relativistic BWT, Tech. Phys. Lett. **25**, 217 (1999).

[11] J. Mitterauer, P. Till, E. Fraunschiel, and M. Haider, The initiation of cathode induced vacuum breakdown by dynamic field emisson (DF-emission) from microprotrusions, in *Proceedings of the VII International Symposium on Discharges and Electrical Insulation in Vacuum, Novosibirsk* (Siberian Branch of Academy of Science of USSR, Novosibirsk, 1976), p. 83.

[12] G. N. Fursey, Field Emission and Vacuum Breakdown, IEEE Trans. Electr. Insul. **EI-20**, 659 (1985).

[13] J. Wang and G. Loew, Report No. SLAC-PUB-7684, 1997.

[14] A. C. Keser, T. M. Antonsen, G. S. Nusinovich, D. G. Kashyn, and K. L. Jensen, Heating of microprotrusions in accelerating structures, Phys. Rev. ST Accel. Beams **16**, 092001 (2013).

[15] H. Timko, K. Ness Sjobak, L. Mether, S. Calatroni, F. Djurabekova, K. Matyash, K. Nordlund, R. Schneider, and W. Wuensch, From field emission to vacuum arc ignition: A new tool for simulating copper vacuum arcs, Contrib. Plasma Phys. **55**, 299 (2015).

[16] A. Anders, *Cathodic Arcs: From Fractal Spots to Energetic Condensation* (Springer, New York, 2008).

[17] K. Eimre, S. Parviainen, A. Aabloo, F. Djurabekova, and V. Zadin, Application of the general thermal field model to simulate the behaviour of nanoscale Cu field emitters, J. Appl. Phys. **118**, 033303 (2015).

[18] E. A. Litvinov, G. A. Mesyats, and D. I. Proskurovskiĭ, Field emission and explosive electron emission processes in vacuum discharges, Phys.-Usp. **26**, 138 (1983).

[19] G. W. Anderson and F. W. Neilson, in *Exploding Wires*, edited by W. G. Chace and H. K. Moore (Plenum, New York, 1962).

[20] J. P. Barbour, W. W. Dolan, J. K. Trolan, E. E. Martin, and W. P. Dyke, Space-charge effects in field emission, Phys. Rev. **92**, 45 (1953).

[21] A. Descoeudres, Y. Levinsen, S. Calatroni, M. Taborelli, and W. Wuensch, Investigation of the dc vacuum breakdown mechanism, Phys. Rev. ST Accel. Beams **12**, 092001 (2009).

[22] S. A. Barengolts, M. Y. Kreindel, and E. A. Litvinov, Initiation of explosive electron emission in microwave fields, IEEE Trans. Plasma Sci. **26**, 252 (1998).

[23] V. G. Pavlov, A. A. Rabinovich, and V. N. Shrednik, High local density currents of stationary field emission, Sov. Phys. Tech. Phys. **20**, 1337 (1975).

[24] *A Multi-TeV Linear collider Based on CLIC Technology: CLIC Conceptual Design Report*, edited by M. Aicheler, P. Burrows, M. Draper, T. Garvey, P. Lebrun, K. Peach, N. Phinney, H. Schmickler, D. Schulte, and N. Toge (CERN Report No. CERN-012-007, 2012).

[25] D. P. Pritzkau and R. H. Siemann, Experimental study of rf pulsed heating on oxygen free electronic copper, Phys. Rev. ST Accel. Beams **5**, 112002 (2002).

[26] J. Shi, H. Chen, A. Grudiev, W. Wuensch, B. Spataro, Y. Higashi, and V. Dolgashev, New quantity describing the pulse shape dependence of the high gradient limit in single cell standing-wave accelerating structures, in *The 7th International Particle Accelerator Conference, (IPAC'16), Busan, Korea, 2016*, p. 3878, DOI: 10.18429/JACoW-IPAC2016-THPOR042, http://jacow.org/ipac2016/papers/thpor042.pdf.

[27] E. I. Simakov, V. A. Dolgashev, and S. G. Tantawi, Advances in high gradient normal conducting accelerator structures, Nucl. Instrum. Methods Phys. Res., Sect. A, DOI: 10.1016/j.nima.2018.02.085 (2018).

[28] D. G. Sokolovski and L. M. Baskin, Traversal time in quantum scattering, Phys. Rev. A **36**, 4604 (1987).

[29] G. N. Fursey, *Field Emission in Vacuum Microelectronics* (Springer Science & Business Media, New York, 2007).

[30] J. W. Wang and G. A. Loew, in *Frontiers of Accelerator Technology* (World Scientific, Singapore, 1999), p. 768.

[31] I. V. Uimanov, The dimensional effect of the space charge on the self-consistent electric field at the cathode surface, IEEE Trans. Dielectr. Electr. Insul. **18**, 924 (2011).

[32] S. I. Shkuratov, S. A. Barengolts, and E. A. Litvinov, Heating and failure of niobium tip cathodes due to a high-density pulsed field electron emission current, J. Vac. Sci. Technol. B **13**, 1960 (1995).

[33] G. A. Mesyats and I. V. Uimanov, Numerical simulation of vacuum prebreakdown phenomena in a cathode microprotrusion at subnanosecond pulse durations, in *Proceedings of the XXIII International Symposium on Discharges and Electrical Insulation in Vacuum, Bucharest, Romania, 2008*, Vol. 1 (IEEE , 2008), p. 17.

[34] V. V. Loskutov, A. V. Luchinskii, and G. A. Mesyats, Magnetohydrodynamic processes in the initial stage of explosive emission, Sov. Phys. Dokl. **28**, 654 (1983).

[35] A. V. Bushman, S. L. Leshkevich, G. A. Mesyats, V. A. Skvortsov, and V. E. Fortov, Mathematical modeling of an electric explosion of a cathode micropoint, Sov. Phys. Dokl. **35**, 561 (1990).

[36] D. L. Shmelev and E. A. Litvinov, The computer simulation of the vacuum arc emission center, IEEE Trans. Plasma Sci. **25**, 533 (1997).

[37] D. L. Shmelev and E. A. Litvinov, Computer simulation of ecton in a vacuum arc, IEEE Trans. Dielectr. Electr. Insul. **6**, 441 (1999).

[38] S. Barengolts, G. Mesyats, and D. Shmelev, Mechanism of ion flow generation in vacuum arcs, J. Exp. Theor. Phys. **93**, 1065 (2001).

[39] V. I. Oreshkin, R. B. Baksht, N. A. Ratakhin, A. V. Shishlov, K. V. Khishchenko, P. R. Levashov, and I. I. Beilis, Wire explosion in vacuum: Simulation of a striation appearance, Phys. Plasmas **11**, 4771 (2004).

[40] V. I. Oreshkin, S. A. Chaikovsky, I. M. Datsko, N. A. Labetskaya, G. A. Mesyats, E. V. Oreshkin, N. A. Ratakhin, and D. V. Rybka, MHD instabilities developing in a conductor exploding in the skin effect mode, Phys. Plasmas **23**, 122107 (2016).

[41] V. E. Fortov, K. V. Khishchenko, P. R. Levashov, and I. V. Lomonosov, Wide-range multi-phase equations of state for metals, Nucl. Instrum. Methods Phys. Res., Sect. A **415**, 604 (1998).

[42] V. I. Oreshkin, R. B. Baksht, A. Yu. Labetskii, A. G. Russkikh, A. V. Shishlov, P. R. Levashov, K. V. Khishchenko, and I. V. Glazyrin, Study of metal conductivity near the critical point using a microwire electrical explosion in water, Tech. Phys. **49**, 843 (2004).

[43] G. A. Mesyats and I. V. Uimanov, Hydrodynamics of the molten metal during the crater formation on the cathode surface in a vacuum arc, IEEE Trans. Plasma Sci. **43**, 2241 (2015).

[44] H. T. Kaufmann, M. D. Cunha, M. S. Benilov, W. Hartmann, and N. Wenzel, Detailed numerical simulation of cathode spots in vacuum arcs: Interplay of different mechanisms and ejection of droplets, J. Appl. Phys. **122**, 163303 (2017).

[45] X. Zhang, L. Wang, S. Jia, and D. L. Shmelev, Modeling of cathode spot crater formation and development in vacuum arc, J. Phys. D **50**, 455203 (2017).

[46] H. Timko *et al.*, Mechanism of surface modification in the plasma-surface interaction in electrical arcs, Phys. Rev. B **81**, 184109 (2010).

[47] F. Djurabekova, J. Samela, H. Timko, K. Nordlund, S. Calatroni, M. Taborelli, and W. Wuensch, Crater formation by single ions, cluster ions and ion "showers", Nucl. Instrum. Methods Phys. Res., Sect. B **272**, 374 (2012).

[48] E. D. Korop and A. A. Plyutto, Acceleration of ions of cathode material in vacuum breakdown, Sov. Phys. Tech. Phys. **15**, 1986 (1970).

[49] D. I. Proskurovskii, V. P. Rotshtein, A. F. Shubin, and E. B. Yankelevich, Processes in vacuum diode during a cathode burst, Sov. Phys. Tech. Phys. **20**, 1342 (1975).

[50] S. A. Barengol'ts, G. A. Mesyats, and E. A. Perel'shtein, Model of collective ion acceleration in a vacuum discharge based on the concept of a deep potential well, J. Exp. Theor. Phys. **91**, 1176 (2000).

[51] B. Jüttner, W. Rohrbeck, and H. Wolff, Zerstörung und Erzeugung von Feldemittern auf ausgedehnten Metalloberflächen, Beitrage aus der Plasmaphysik **10**, 383 (1970).

[52] E. Hantzsche, B. Jüttner, V. F. Puchkarov, W. Rohrbeck, and H. Wolff, Erosion of metal cathodes by arcs and breakdowns in vacuum, J. Phys. D **9**, 1771 (1976).